Bull. Mater. Sci., Vol. 38, No. 7, December 2015, pp. 1891–1897. © Indian Academy of Sciences.

Low resistivity molybdenum thin film towards the back contact of dye-sensitized solar cell

VUONG SON[1], TRAN THI HA[1], LUONG T THU THUY[2,*], NGUYEN NGOC HA[2], NGUYEN DUC CHIEN[1] and MAI ANH TUAN[1]

[1]International Training Institute for Materials Science (ITIMS), Hanoi University of Science and Technology, No. 1 Dai Co Viet Road, Hanoi, Viet Nam

[2]Department of Chemistry, Hanoi National University of Education, 136 Xuan Thuy Street, Hanoi, Viet Nam

MS received 21 November 2014; accepted 6 July 2015

Abstract. This paper reports the optimization of the molybdenum thin film electrode as the back contact of dye-sensitized solar cell (DSSC). The molybdenum thin film was grown on the glass substrate by direct current sputtering techniques of which the sputtering power was 150 W at 18 sccm flow rate of Ar. At such sputtering parameters, the Mo film can reach the lowest resistivity of 1.28E−6 Ω cm at 400 nm thick. And the reflection of Mo membrane was 82%. This value is considered as a very good result for preparation of the back contact of DSSC.

Keywords. Back contact; molybdenum; DC sputtering; dye-sensitized solar cell.

1. Introduction

The Sun offers Earth more than 1 kW m^{-2} but the maximum energy that people can harvest is 25.6%.[1] To date, the silicon-based technology is still dominant in solar cell production.[2] The silicon solar cell benefits from the silicon and semiconductor technology, the mature processes that require the use of clean room and high thermal treatment during the fabrication. Much effort has been made, on one hand; to reduce the raw material consumption in cell production, on the other hand; to enhance the efficiency of the solar cell.[3–6] However, using expensive raw material and clean process together with high thermal treatment makes it high cost of production; and leads to the limitation in application of silicon solar cell.

Dye-sensitized solar cell (DSSC) is considered as the alternative choice for the conventional technology due to the advantages of low cost and ease of fabrication from stable and abundant materials.[7] In comparison with silicon-based cells, the DSSC has the ability to absorb more radiation per area. The flexible cells can be implemented for various applications that are not applicable in rigid silicon cells. In addition, for the last decade, the scientists and engineers have tried to narrow the gap in cell efficiency with that of silicon solar cell[2,8,9] by overcoming the obstacles in preparation of the materials and every single fabrication processes.[10–14]

A typical DSSC consists of a nanocrystalline TiO_2 layer in conjunction with the dye prepared on a transparent conducting oxide (TCO), a metal counter electrode and an electrolyte solution redox couple between the electrodes (figure 1). The dye works as a photon adsorption and, incorporation with the TiO_2 layer, converts the solar radiation into electron current. The back contact, a thin layer of metal covers the entire back surface of the cell.

The back contact, at the electronics of charge-separating interfaces contributes in the reduction of the energy losses associated with exciton dissociation, charge separation, and collection, works as a conductor that needs to be thin and low resistive so that the charge can be accumulated to create a better current density which contributes to better efficiency of the solar cell.

In order to collect the carriers from the dyes, the Ohmic contact is required at the back of a DSSC. For this purpose, a number of metals have been investigated so far as Cu,[15] Pt,[16,17] Mo,[18–20] Ni[21] or, in recent times, the conductive materials as conducting polymer[22] carbon nanotube and graphene,[23,24] cobalt sulphide[25] and composite film.[26,27] Among them, molybdenum meets most requirements in solar cell production. Mo offers an inert properties in deposition process; large grain[28,29] via an intermediate $MoSe_2$ layer.[30] This metal allows the Ohmic contact in DSSC or copper–zinc–tin–sulphur–selenium (CZTSSe) that leads to a formation of an interfacial layer Mo–Se in between during the thermal treatment. Thus, molybdenum does not only work as a back contact but also like a chemical barrier.[31] The performance of copper indium gallium (di)selenide (CIGS), especially the open-circuit, can be significantly improved by a small amount of sodium in the absorber. The diffusion trace of sodium can be controlled by modifying the molybdenum layer thickness, the grain density, and by a diffusion barrier to the glass.[32]

*Author for correspondence (hihithuy@gmail.com)

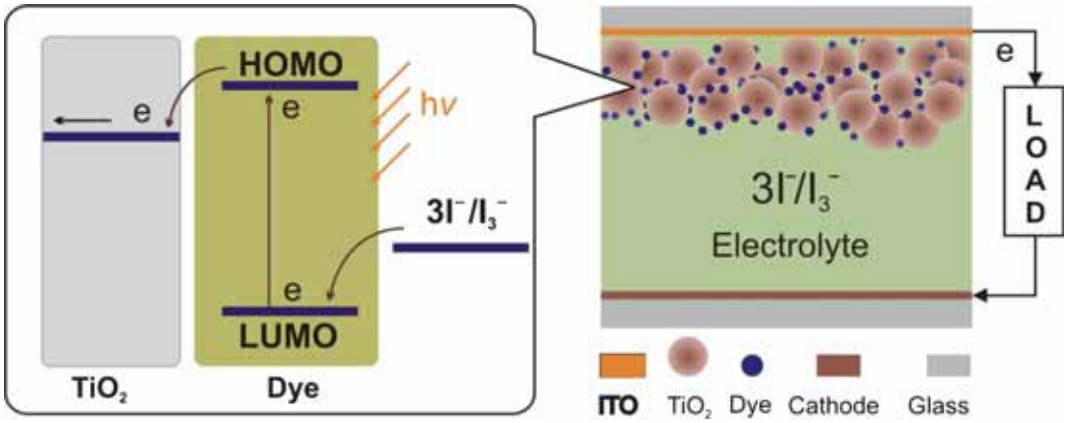

Figure 1. Structure and operation mechanism of a DSSC.

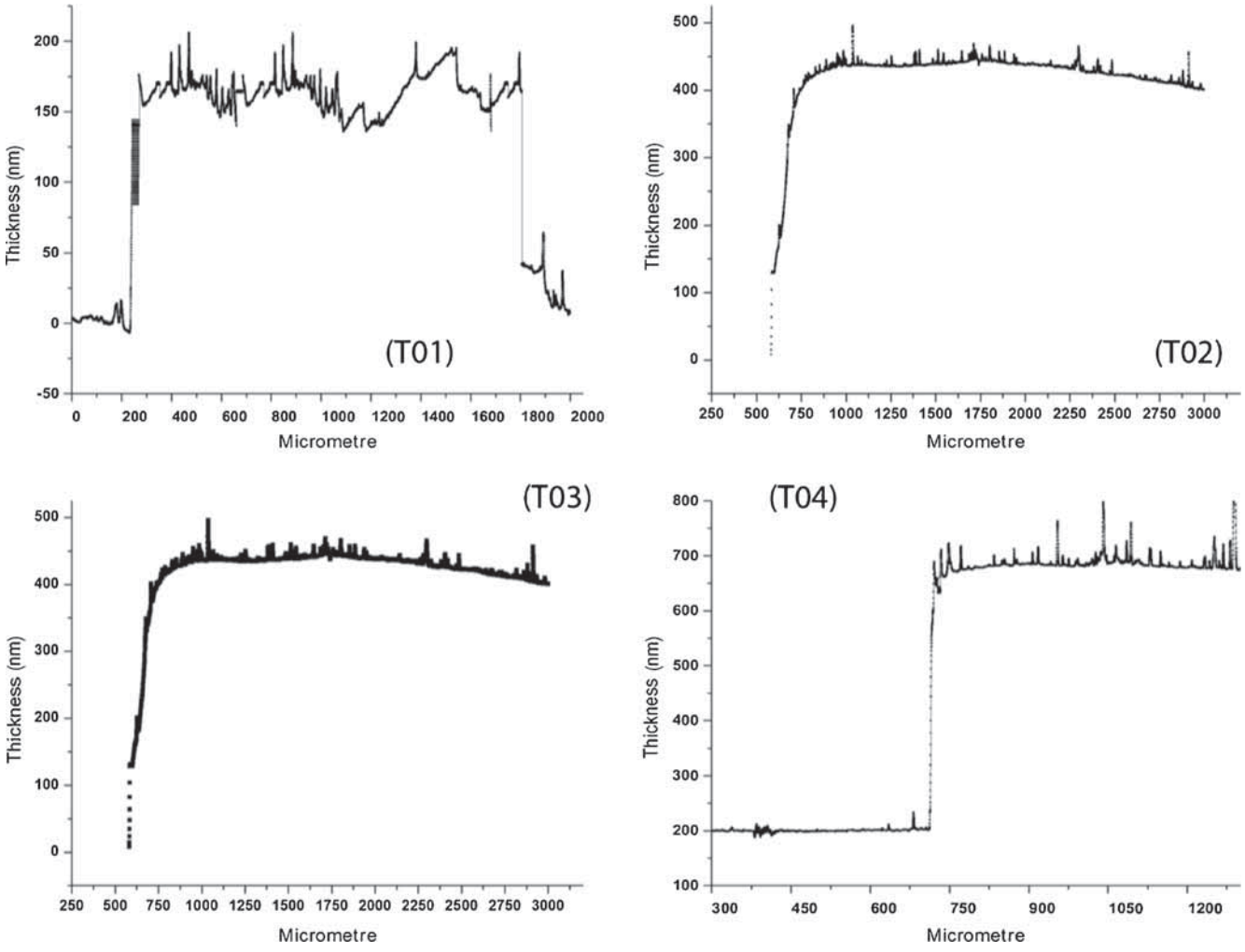

Figure 2. Mo layers were obtained by using the DC sputtering technique at different sputtering times. The base vacuum was 1E−6 mbar, the sputtering vacuum was 10 mbar; the sputtering power was 150 W. The average sputtered rate was 9.95 nm min^{-1}.

Molybdenum can be obtained by pulse direct current magnetron sputtering,[33] thermal evaporation[34] and e-beam evaporation.[35] The DC sputtering is considered a suitable technique for deposition of Mo membrane of which will meet the requirements in solar cell development.

2. Experimental

2.1 *Materials and apparatus*

Briefly, 2″ in diameter, 99.99% Mo target (Semiconductor Wafer Inc., Taiwan), soda lime glass (SLG) as sputtering

substrate, sulphuric acid 98%, acetone and isopropanol (IPA) from Merck.

DC sputtering machine, SIEMENS D5005, surface profilometer (Veeco Dektak 150), Jasco V530UV–Vis/NIR, scanning electron microscope S4800-Hitachi; the four-point probe RM3000 Test Unit from Bridge Technology USA.

2.2 *Experiment set-up*

Before the sputtering process, the substrate surface needs to be chemically treated in order to remove the defect and enhance the adhesion. The SLG substrate was dipped; with ultrasonic assisted, in sulphuric acid for 30 min followed by cleaning by acetone; IPC and de-ionized water. Then, it was dried by blown nitrogen and attached on the substrate holder.

Before every coating process, the target was clean by pre-sputtering in 5 min to remove the native oxide layer on the substrate surface. A Cr thin film as lining layer was used to enhance the adhesion of Mo thin film to SLG substrate. The sputtering power (100, 150, 200, 250 W), the flow rate of argon (18, 20, 26, 30 sccm), the sputtering time (9, 16, 38, 44, 72 min) and the thin film's thickness was investigated to evaluate their influence to the electrical and optical properties of the Mo thin film. The substrate temperature was kept constant, the distance between target and substrate was fixed at 25 cm, the basic vacuum was set at 1.E−6 mbar and the sputtered vacuum was 10 mbar.

Because a series of experiments were carried out, to investigate the influence of technological factors, only one deposition parameter was changed at a time while keeping all other conditions unchanged.

The thickness of the Mo layer was determined by the Veeco Dektak 150 surface profilometer, the morphology was investigated using Hitachi SEM S4800. The XRD spectrum was performed by SIEMENS D5005 with copper anode ($\lambda = 1.54056$ Å), scan step 0.02°, step time 1.0 s, and at room temperature.

The sheet resistance range of the RM3000 Test Unit is from 1 mΩ square^{-1} (10^{-3}) up to 5×10^8 Ω square^{-1} with 0.3% accuracy. The volume resistivity range is from 1 mΩ cm (10^{-3}) up to 10^6 Ω cm. This range refers to measuring a bulk material directly as opposed to measuring a thin film and converting to volume resistivity using the built-in software. And, the optical properties of the thin film were measured by Jasco V530UV–Vis/NIR Spectrophotometer.

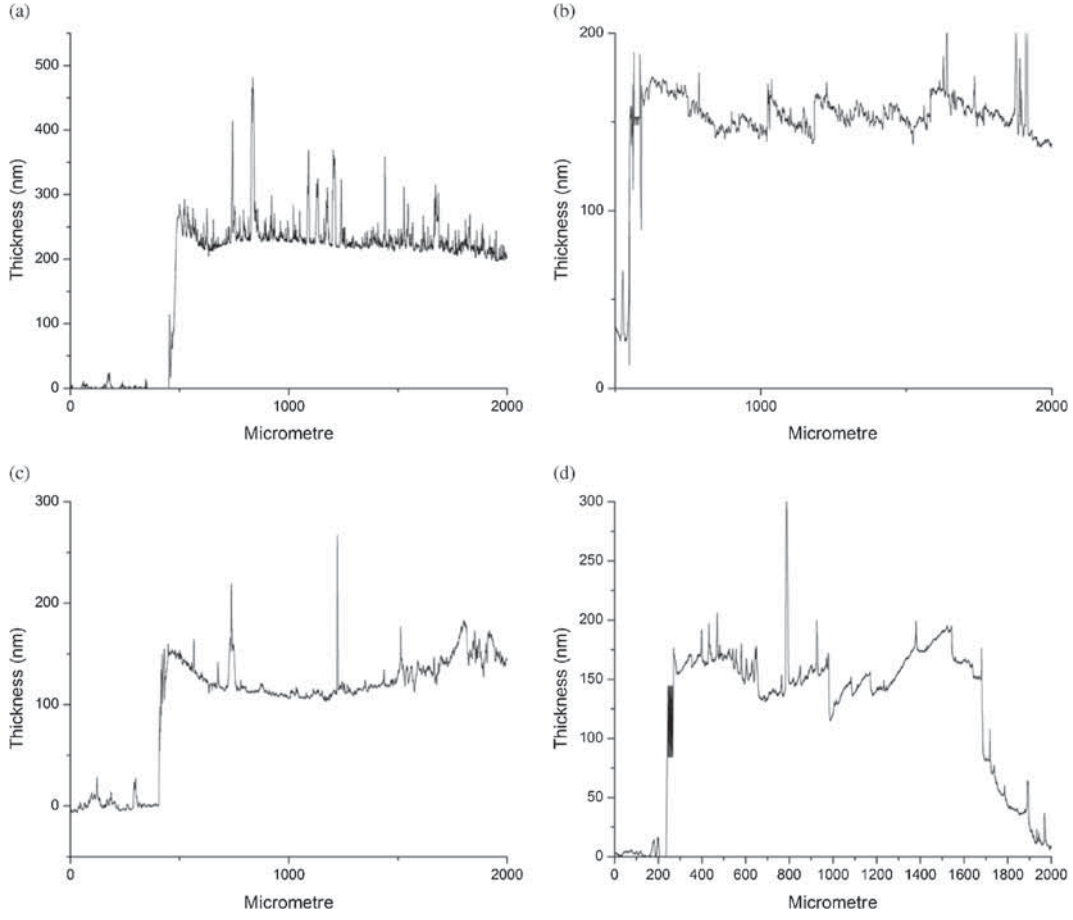

Figure 3. Thickness of Mo film obtained by different sputtering powers (including 35 nm of chromium as lining layer): (**a**) $P = 100$ W; (**b**) $P = 150$ W; (**c**) $P = 200$ W and (**d**) $P = 250$ W. The base vacuum was 1E−6 mbar, the sputtering vacuum was 10 mbar; the sputtering time was 10 min.

3. Results and discussion

3.1 *The sputtered rate and the thickness of the Mo thin film*

The sputtered rate was empirically calculated by using the dummy layer. The sputtering time was set at 9, 18, 36, 44 and 72 min. As can be seen in figure 2, the obtained thickness is 100, 200, 400, 600 and 800 nm, respectively. These values include 30 nm of the Cr lining layer.

The surface profiles of Mo thin films in figure 2c and d are both smooth and fine because the grains on thin film's surface are small enough in comparison with the thickness of the film. However, a thicker film requires more material, more power, and takes longer time. For a suitable thickness value, the average sputtered rate was set at 9.95 nm min^{-1} and the final thickness would be 400 nm.

3.2 *Sputtering power*

The deposition speed at different DC powers can be calculated based on the thickness of the film (obtained by the surface profilometer) by using following equation:

$$S = \tau/t, \tag{1}$$

where s is the deposition rate (nm min^{-1}); τ the thickness (nm); t the deposition time (min).

As illustrated in figure 3, at 100 and 150 W sputtering power, the surface profiles of Mo thin films are uniform and stable with the average peaks' height smaller than 50 nm. At $P = 150$ W, peaks are smooth, the film's surface is uniform, and no large drain observed. At $P = 200$ W, film surface becomes less smooth. The film's surface becomes very unstable with big amplitude of fluctuation. The thickness changes from 110 to 150 nm along a path of 1500 nm long. When the sputtering power was set at 250 W, the film's thickness is not uniform over the entire sputtering area.

As depicted in figure 3, the surface morphologies of Mo films obtained by different DC powers are indicatives of evolving microstructures at various stages of film growth by the scanning electron microscope image.

In figure 4, the similar morphology of the Mo layers, deposited at 100 and 150 W, is honeycomb and randomly oriented crystallites. The layers grown at 200 W had strip structure incorporation with conglomerates in large dimension (figure 4c). The layers, obtained at 250 W, had smooth surfaces but cracks of 150–750 nm widths appeared which may be caused by the internal stress (figure 4d). The applied energy for the bombarding particles in this case was sufficient to grow a highly oriented crystal structure.

3.3 *Flow rate of argon*

Varying the argon flow means changing the working pressure in sputtering chamber or changing the deposition rate of the Mo membrane. Lower pressure corresponds to longer mean free path, less collisions of the sputtered particle with the gas and therefore leads to higher deposition rate. Due to this reason, the sputtered particles will reduce the arrival

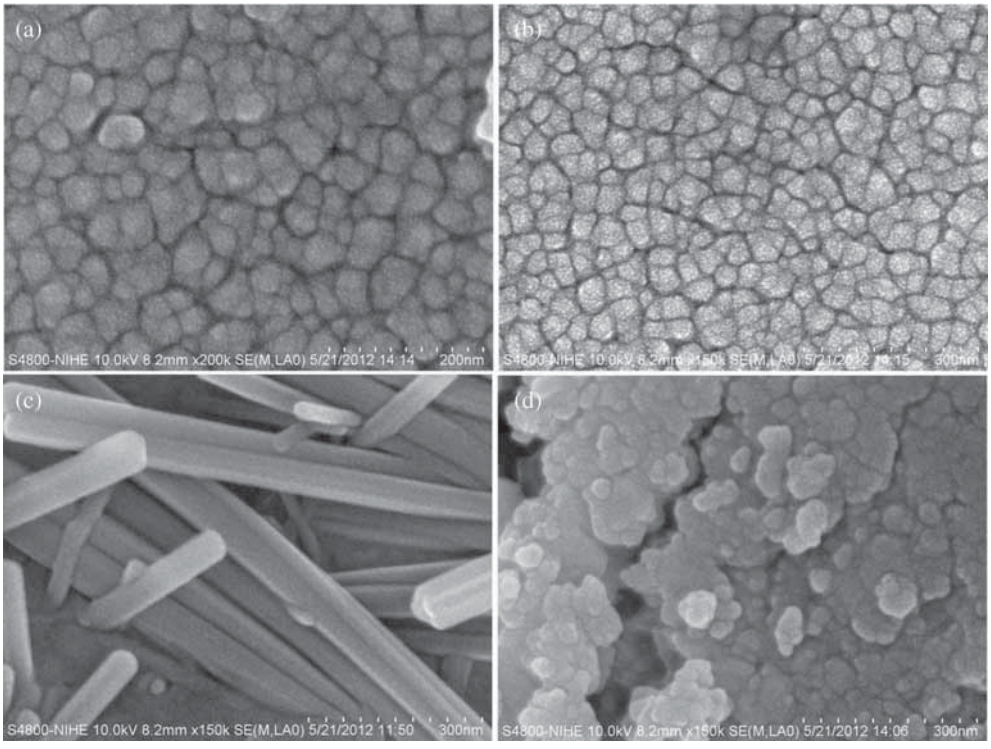

Figure 4. Scanning electron microscope images of deposited Mo thin films formed with different sputtering powers: (**a**) 100 W; (**b**) 150 W; (**c**) 200 W and (**d**) 250 W.

angles to the substrate. Thus, the possibility of the formation of inter-granule void reduced, which, in turn, results in the dense structure of the grains and hence the improvement in the crystal size of the films to be increased. At a higher pressure (higher Ar flow), due to the multiple collisions of the sputtered particles with the gas, the deposition rate is reduced and the crystal size is decreased.

At fixed sputtering power and desired thickness of thin film (400 nm), lowering the deposition rate will result in smoother film. However, very low sputtering rate will require a longer sputtering time.

In figure 5, the deposition rate of Mo varies about 10% when the Ar flow was changed from 18 sccm (11.9 nm min^{-1}) to 30 sccm (9.8 nm min^{-1}). Other investigation shows that the argon flow rate at 18 sccm contributed good results as smoother surface, lower resistance and higher reflectivity.

3.4 *Dependence of microstructure of Mo film on argon flow rate*

The X-ray diffraction of Mo thin films deposited at different argon flow rates is in good matching with (110) planes with the JCPDS data card 01-1208 (figure 6). Using the values of the full-width half-maxima (FWHM) and Scherrer's formula, the crystallite size (D) was 3.48 nm at high argon flow rate and increased to 21.04 nm for the low argon flow rate. In this work, as depicted in figure 6 (small one) the suitable flow rate of argon is 18 sccm.

3.5 *Electrical properties of Mo thin films*

The electrical properties of 400 nm Mo thin films measured by four-point probe are listed in table 1. The lowest resistivity was 10.52E−06 Ω cm (at 1 mA applied current) when the sputtering power 150 W.

3.6 *Optical property of the Mo membrane*

It is known that more light in a solar cell structure more electron–hole pairs created, leading to a better efficiency. In this work, the Mo thin films obtained by implying different sputtering parameters were examined using the UV–vis spectroscopy. The results show that smaller sputtering power will provide a better reflection (figure 7a). However, the smallest power means that the sputtering process takes longest to gain 400 nm thick. In accordance with the above discussion about the sputtering powers, in this work, 150 W is found

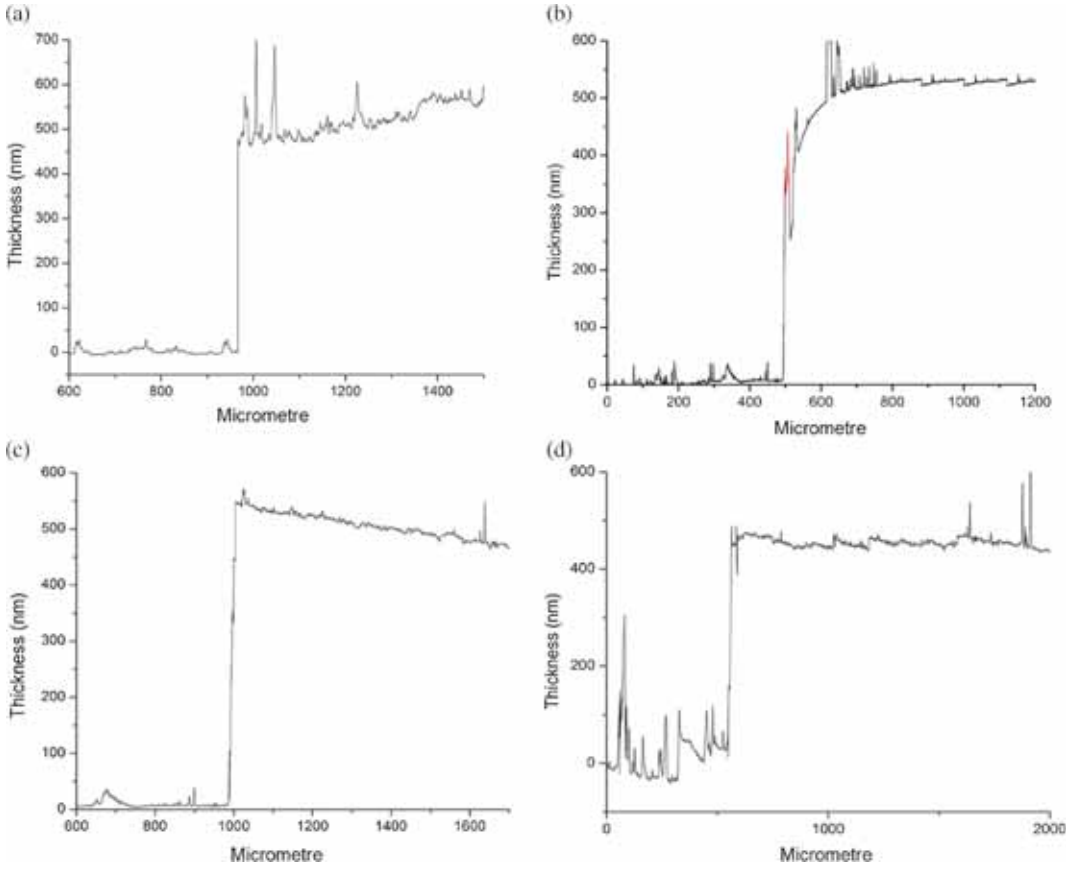

Figure 5. Thickness and surface profile of samples obtained by DC sputtering at different Ar flows: (**a**) 18 sccm; (**b**) 22 sccm; (**c**) 26 sccm and (**d**) 30 sccm.

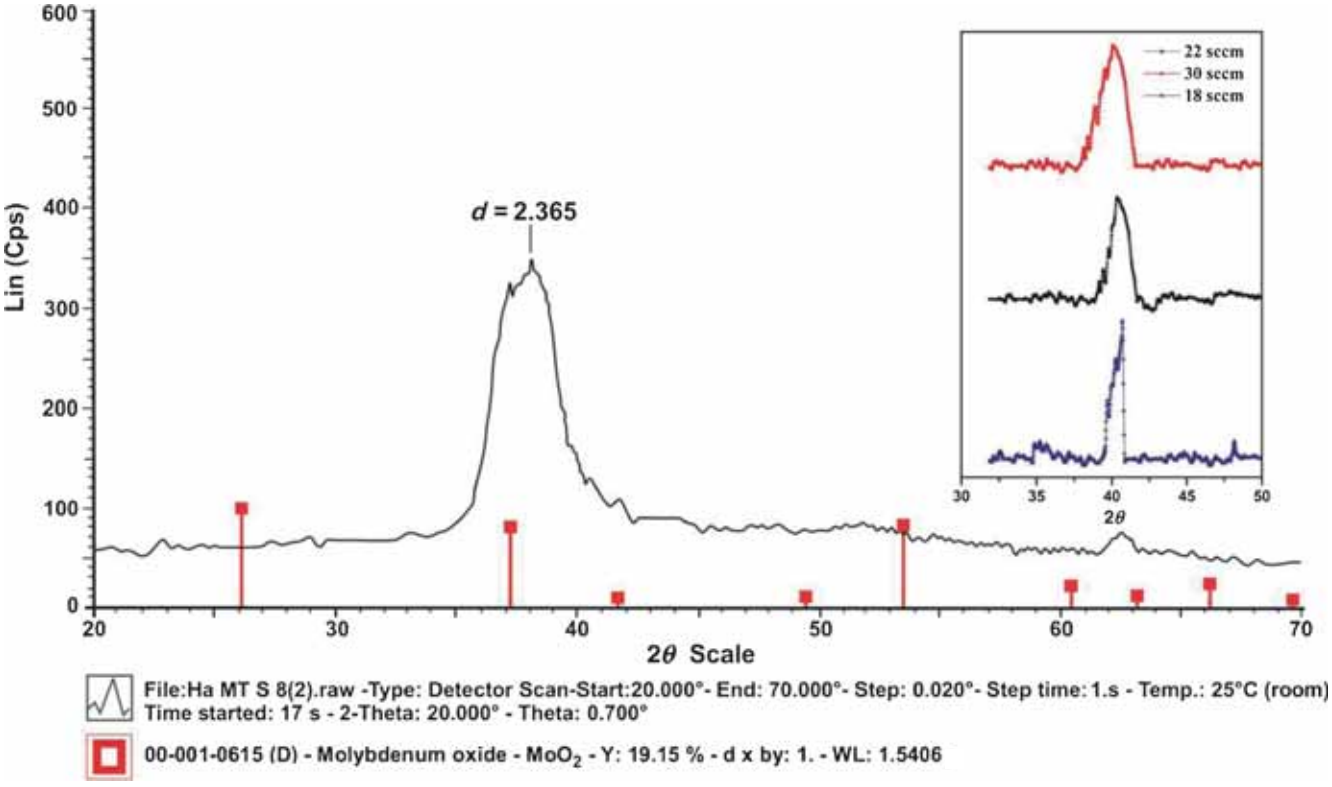

Figure 6. XRD pattern of obtained Mo membrane. The working pressure was at 18 sccm (the results are the same for 22 and 30 sccm, data not shown). The DC sputtering power was 150 W and the total thickness was 400 nm.

Table 1. Electrical properties of the thin films as measured by four-point probe.

No. 1	P (W)	R (Ω cm^{-2})	V (mV)	Thickness (nm)	ρ (Ω cm)
P01	100	18.1	8.796	400	72.4E−05
P02	150	0.262879	0.058	400	1.052E−05
P03	200	0.285541	0.063	400	1.142E−05
P04	250	0.593744	0.131	400	2.375E−05

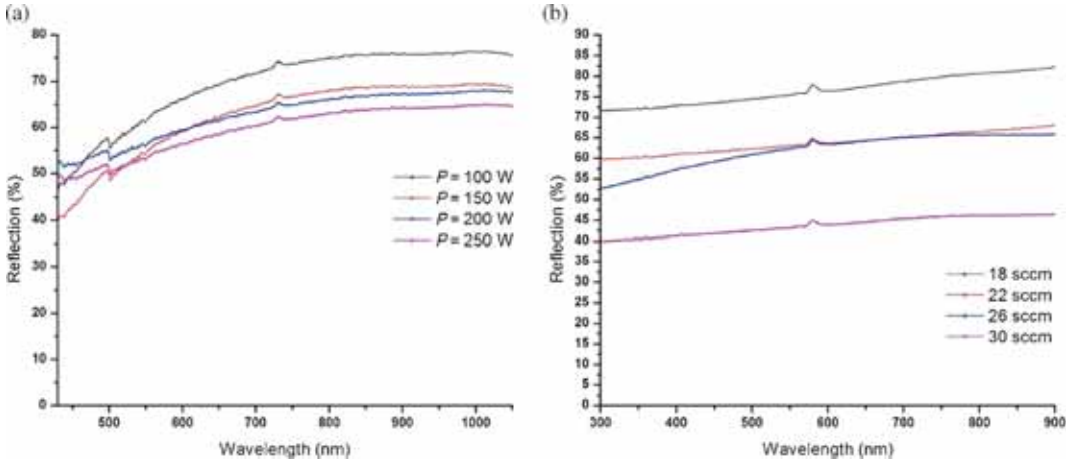

Figure 7. Reflection of the Mo membrane (including 35 nm of Cr layer) depends on: (**a**) the sputtering power and (**b**) the flow rate of Ar. The base vacuum was 1E−6 mbar, the working vacuum was 10 mbar; the sputtering time was 10 min.

to be a suitable value for Mo sputtering process. Figure 7b also presents a matching result with previous discussion in which 18 sccm is suitable flow rate of Ar for Mo membrane formation.

The obtained Mo thin film can reflect 82% of the incident light in the visible range. This value is considered as facilitating factor for a back contact of the DSSC.

4. Conclusion

The development of the Mo membrane, by using DC sputtering technique, towards the back contact electrode of a DSSC is reported in this work. So far, the optimal DC sputtering parameters for Mo deposition are 150 W sputtering power; 18 sccm of argon flow; 1E−6 mbar base vacuum; 10 mbar working vacuum; and 30 min sputtering time. At such conditions, the lowest resistivity of the Mo film can reach 1.28E−6 Ω cm and the reflection of Mo membrane can reach 82% that is considered as very good value for back contact in DSSC. Further study is needed for better understanding the electrical behaviour at the Mo junction and the cell.

Acknowledgement

This work was financially supported by the Vietnamese National Foundation for Science and Technology Development (NAFOSTED) for a basic research project (104.99-2011.44 code).

References

1. Panasonic Press Release 2014 *Panasonic HIT®solar cell achieves world's highest energy conversion efficiency of 25.6% at research level*
2. Green M A, Emery K, Hishikawa Y, Warta W and Dunlop E D 2015 *Prog. Photovolt: Res. Appl.* **23** 1
3. Chen Y H, Liu Y T, Huang C F, Liu J C and Lin C C 2015 *Mater. Sci. Semicond. Proc.* **31** 184
4. Lin C C, Chuang Y J, Sun W H, Cheng C, Chen Y T, Chen Z L, Chien C H and Ko F H 2015 *Microelectron. Eng.* **145** 128
5. Liu Y, Zi W, Liu S and Yan B 2015 *Sol. Energy Mater. Sol. Cells* **140** 180
6. Chowdhury A, Kang D W, Isshiki M, Oyama T, Odaka H, Sichanugrist P and Konagai M 2015 *Sol. Energy Mater. Sol. Cells* **140** 126
7. O'Regan B and Grätzel M 1991 *Nature* **353** 737
8. Vougioukalakis G C, Philippopoulos A I, Stergiopoulos T and Falaras P 2011 *Coord. Chem. Rev.* **255** 2602
9. Grätzel M 2009 *Acc. Chem. Res.* **42** 1788
10. Shoyebmohamad F S, Rajaram S M, Hwang Y J and Joo O S 2015 *Electrochim. Acta* **167** 379
11. Wang G, Zhang J, Kuang S and Zhuo S 2015 *Mater. Sci. Semicond. Proc.* **38** 234
12. Arbab A A, Sun K C, Sahito I A, Qadir M B and Jeong S H 2015 *Appl. Surf. Sci.* **349** 174
13. Robertson N 2006 *Angew. Chem. Int. Ed.* **45** 2338
14. Wu J H, Lan Z, Lin J M, Huang M L, Hao S C, Sato T and Yin S 2007 *Adv. Mater.* **19** 4006
15. Korevaar B A, Shuba R, Yakimov A, Cao H, Rojo J C and Tolliver T R 2011 *Thin Solid Films* **519** 7160
16. Lee K M, Lin L C, Chen C Y, Suryanarayanan V and Wu C G 2014 *Electrochim. Acta* **135** 578
17. Son M K, Seo K, Kim S K, Hong N Y, Kim B M, Park S, Prabakar K and Kim H J 2013 *J. Power Sources* **222** 333
18. Gautron E, Tomassini M, Arzel L and Barreau N 2012 *Surf. Coat. Technol.* **211** 29
19. Wu H M, Liang S C, Lin Y L, Ni C Y, Bor H Y, Tsai D C and Shieu F S 2012 *Vacuum* **86** 1916
20. Su C Y, Liao K H, Pan C T and Peng P W 2012 *Thin Solid Films* **520** 5936
21. Park S H, Cho Y H, Choi M, Choi H, Kang J S, Um J H, Choi J W, Choe H and Sung Y E 2014 *Surf. Coat. Technol.* **259** 560
22. Saranya K, Rameez M and Subramania A 2015 *Eur. Polym. J.* **66** 207
23. Bi H, Cui H, Lin T and Huang F 2015 *Carbon* **91** 153
24. Selopal G S, Milan R, Ortolani L, Morandi V, Rizzoli R, Sberveglieri G, Veronese G P, Vomiero A and Concina I 2015 *Sol. Energy Mater. Sol. Cells* **135** 99
25. Chae S Y, Hwang Y J, Choi J H and Joo O S 2013 *Electrochim. Acta* **114** 745
26. Zheng M, Huo J, Tu Y, Wu J, Hu L and Dai S 2015 *Electrochim. Acta* **173** 252
27. Bu I Y Y and Zheng J 2015 *Mater. Sci. Semicond. Proc.* **39** 223
28. Shafarman W N and Phillips J E 1996 *Proceedings of the 25th IEEE photovoltaic specialists conference* (Washington, DC: IEEE) p 917
29. Orgassa K, Schock H W and Werner J H 2003 *Thin Solid Films* **431–432** 387
30. Wada T, Kohara N, Negami T and Nishitani M 1996 *Jpn. J. Appl. Phys.* **35** L1253
31. Wada T, Kohara N, Nishiwaki S and Negami T 2001 *Thin Solid Films* **387** 118
32. Rockett A 2005 *Thin Solid Films* **480–481** 2
33. Karthikeyan S, Hill A E and Pilkington R D 2011 *Thin Solid Films* **520** 266
34. Paudel N R, Compaan A D and Yan Y 2013 *Sol. Energy Mater. Sol. Cells* **113** 26
35. Martinez M A and Guillén C 2003 *J. Mater. Process. Technol.* **143–144** 3263